

Strong Uniaxial Magnetic Anisotropy in CoFe films on  
Obliquely Sputtered Ru Underlayer

G. Mankey – University of Alabama

et al.

Deposited 07/09/2019

Citation of published version:

Fukuma, Y., et al. (2009): Strong Uniaxial Magnetic Anisotropy in CoFe films on  
Obliquely Sputtered Ru Underlayer. *Journal of Applied Physics*, 106(7).

DOI: <https://doi.org/10.1063/1.3223538>

# Strong uniaxial magnetic anisotropy in CoFe films on obliquely sputtered Ru underlayer

Cite as: J. Appl. Phys. **106**, 076101 (2009); <https://doi.org/10.1063/1.3223538>

Submitted: 03 June 2009 . Accepted: 12 August 2009 . Published Online: 02 October 2009

Y. Fukuma, Z. Lu, H. Fujiwara, G. J. Mankey, W. H. Butler, and S. Matsunuma



View Online



Export Citation

## ARTICLES YOU MAY BE INTERESTED IN

[Controlling the anisotropy and domain structure with oblique deposition and substrate rotation](#)

AIP Advances **4**, 027104 (2014); <https://doi.org/10.1063/1.4865248>

[Surface morphology and magnetic anisotropy of obliquely deposited Co/Si\(111\) films](#)

Applied Physics Letters **97**, 022507 (2010); <https://doi.org/10.1063/1.3463458>

[Uniaxial magnetic anisotropy in cobalt films induced by oblique deposition of an ultrathin cobalt underlayer](#)

Applied Physics Letters **87**, 082505 (2005); <https://doi.org/10.1063/1.2032592>

The advertisement banner features the Alluxa logo on the left, which consists of a stylized 'A' made of three overlapping circles in blue, red, and yellow. To the right of the logo, the text 'Alluxa' is written in a large, white, sans-serif font. Further right, the text 'YOUR OPTICAL COATING PARTNER' is written in a smaller, white, sans-serif font. On the far right, there is a blue rectangular button with a white right-pointing arrow and the text 'DOWNLOAD THE LIDAR WHITEPAPER' in white, sans-serif font.

## Strong uniaxial magnetic anisotropy in CoFe films on obliquely sputtered Ru underlayer

Y. Fukuma,<sup>1,a)</sup> Z. Lu,<sup>1</sup> H. Fujiwara,<sup>1</sup> G. J. Mankey,<sup>1</sup> W. H. Butler,<sup>1</sup> and S. Matsunuma<sup>2</sup>

<sup>1</sup>MINT Center, University of Alabama, Tuscaloosa, Alabama 35487, USA

<sup>2</sup>Hitachi Maxell Ltd., R&D Division, 1-1-88 Ushitora, Ibaraki, Osaka 567-8567, Japan

(Received 3 June 2009; accepted 12 August 2009; published online 2 October 2009)

Co<sub>90</sub>Fe<sub>10</sub> films with an in-plane uniaxial magnetic anisotropy have been grown on an obliquely sputtered thin Ru underlayer. The anisotropy field can be increased up to 200 Oe. The hysteresis curves show a very high squareness in the easy axis direction and almost no hysteresis in the hard axis direction, suggesting that the induced uniaxial anisotropy is uniform throughout the films. The switching characteristics of the nanoelements fabricated from the films by e-beam lithography are also investigated. There is no degradation of the magnetic anisotropy after the annealing and lithographical process. © 2009 American Institute of Physics. [doi:10.1063/1.3223538]

It has been recognized that a higher anisotropy is desirable for future high density magnetic recording and high frequency magnetic devices. For the recording medium, L1<sub>0</sub>-CoPt and FePt are attracting much attention because of the strong perpendicular magnetic anisotropy ( $\sim 10^7$  ergs/cm<sup>3</sup>).<sup>1,2</sup> For various magnetoresistive (MR) devices in MR random access memory and head assemblies of the hard disk drive, an in-plane magnetized film with a uniaxial anisotropy is being used. The magnetic anisotropy is induced by applying a magnetic field during the deposition or postannealing. However, the typical anisotropy field ( $H_K$ ) of NiFe is only a few Oe (the anisotropy energy  $K_u$  is  $\sim 10^3$  ergs/cm<sup>3</sup>) and that of CoFe is  $\sim 30$  Oe ( $K_u \sim 10^4$  ergs/cm<sup>3</sup>), implying a difficulty for the future MR device applications.

The oblique deposition of magnetic films is known to induce a high uniaxial magnetic anisotropy.<sup>3,4</sup> The anisotropy is generally associated with the microstructure such as columnar structures tilted toward the deposition incidence.<sup>5-8</sup> However, such a uniaxial anisotropy is deteriorated by annealing because of deformation of the microstructure.<sup>9,10</sup> A high uniaxial anisotropy is also induced by the anisotropic surface roughness of obliquely deposited Ta, Pt, or Co underlayers.<sup>11-14</sup> While the magnetic films are deposited at normal incidence, the magnetostatic coupling arising from the anisotropic undulation of the interface between the underlayer and the magnetic film causes in-plane magnetic anisotropy. The anisotropy may be of technological importance for MR device applications. However, some improvement may be needed in the smoothness of the film surface, the uniformity of the undulation of the interface, and the thermal stability of the obliquely deposited underlayers.

In this paper, we report a strong uniaxial anisotropy of CoFe films with a smooth surface formed on an obliquely sputtered Ru underlayer on a Si (100) substrate. The samples were deposited at room temperature by dc magnetron sputtering with an Ar pressure of 2 mTorr. The base pressure of

our sputtering system was  $\sim 10^{-9}$  Torr. The residual gas was largely hydrogen. The sputtering targets were Co<sub>90</sub>Fe<sub>10</sub> and Ru disks (99.9%). The two targets were set circumferentially around the substrate holder and the incidence angle  $\theta$  was controlled between 0° and 60° by rotating the substrate (see Fig. 1) for the deposition of the Ru underlayer. The CoFe and capping Ru layers were deposited at the normal incidence angle ( $\theta=0^\circ$ ). A typical deposition rate at  $\theta=0^\circ$  was 0.15 nm/min.

Figure 2 shows the incidence angle dependence of  $H_K$  for Si/Ru (2.5 nm)/CoFe (5.0 nm)/Ru (5.0 nm). The magnetization measurements were done by a vibrating sample magnetometer at room temperature. The magnetic easy axis is perpendicular to the angle of incidence, as shown in Fig. 1. The value of  $H_K$  is deduced from the hard axis loop, as shown in the inset. The induced magnetic anisotropy increases with increasing incidence angle. A small hysteresis is seen in the hard axis loop; however, the remanent/saturation magnetization ratio is much smaller than that of the samples with high  $H_K \sim 200$  Oe in the previous reports.<sup>10,14,15</sup>

It is found that the insertion of a few % N<sub>2</sub> gas into the sputtering gas is effective to suppress the hard axis hysteresis. Figure 3 shows the magnetization curves along the easy and hard axes for Si/Ru (2.5 nm)/CoFe (5.0 nm)/Ru (5.0 nm)

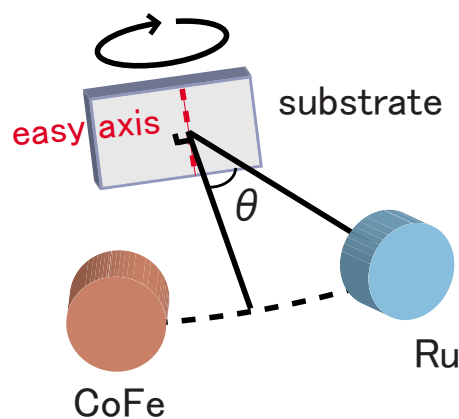


FIG. 1. (Color online) Deposition and anisotropy geometry used in this study.

<sup>a)</sup>Present address: Advanced Science Institute, RIKEN, 2-1 Hirosawa, Wako 351-0198, Japan. Electronic mail: yfukuma@riken.jp.

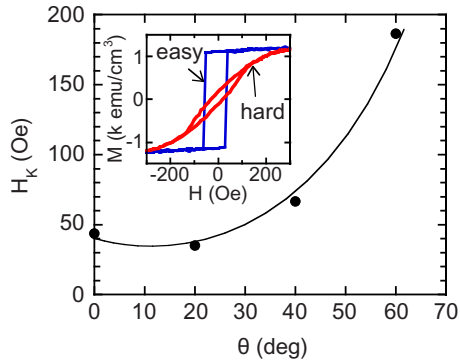


FIG. 2. (Color online) Deposition angle of 5 nm thick Ru underlayer dependence of anisotropy field for 5 nm thick CoFe film. The inset shows the magnetization curves for the sample deposited at  $\theta=60^\circ$ .

deposited at  $\theta=60^\circ$  by adding 3.5%  $N_2$  in Ar. The inset shows the dependence of the normalized remanent magnetization on the angle with respect to the easy axis. The clear  $180^\circ$  symmetry suggests a good uniformity of the uniaxial anisotropy distribution. While  $H_K$  was slightly decreased by inserting  $N_2$  gas, there was no observable change in the saturation magnetization. This may be understood as the effect of the reduction in interface roughness as reported for CoFe on Cu (Ref. 16) and/or that of the grain size reduction itself such as reported for Fe(N) and NiFe films.<sup>17,18</sup> The CoFe thickness dependence of  $H_K$  for the films deposited by using the gas mixture is listed in Table I.  $H_K$  decreased with increasing CoFe thickness.

In order to check the interface, transmission electron microscopy (TEM) and x-ray reflectometry (XRR) were performed. Both experiments revealed a high quality Ru and CoFe interface without significant roughness or atomic mixing.<sup>19</sup> The rms roughness was about 0.4 nm, which is substantially smaller than that in the previous reports.<sup>11,12</sup> Based on Schlomann's analytic calculation,<sup>20</sup>  $H_K$  induced by the anisotropic surface morphology caused by the oblique deposition can be expressed as

$$H_K^* = 2\pi^2 M_S \frac{a^2}{t} \left[ \frac{1}{\lambda_x^2} - \frac{1}{\lambda_y^2} \right] \left[ \frac{1}{\lambda_x^2} + \frac{1}{\lambda_y^2} \right]^{-1/2},$$

where  $M_S$  is the saturation magnetization,  $t$  is the average thickness,  $\lambda_x$  and  $\lambda_y$  are the wavelengths at which the Fourier

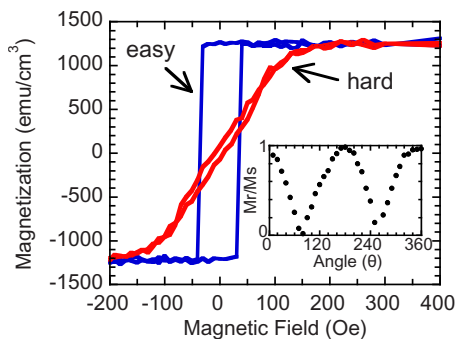


FIG. 3. (Color online) Magnetization curves of 5 nm thick CoFe film on obliquely deposited Ru underlayer at  $\theta=60^\circ$  using Ar+3.5%  $N_2$  gas. The inset shows the remanent magnetization as a function of the angle between the easy axis and the detector.

TABLE I. Summary of CoFe thickness  $t$ , saturation magnetization  $M_S$ , magnetic anisotropy field  $H_K$ , calculated magnetic anisotropy field  $H_K^*$ , uniaxial anisotropy energy  $K_u$ , and activation energy  $K_u V$  for 100 nm element at room temperature.

$t$ (nm)	$M_S$ (emu/cm <sup>3</sup> )	$H_K$ (Oe)	$H_K^*$ (Oe)	$K_u$ (erg/cm <sup>3</sup> )	$K_u V$ ( $k_B T$ )
3	1200	200	230	$1.20 \times 10^5$	68.3
5	1250	130	150	$8.13 \times 10^4$	77.0
10	1400	48	80	$3.36 \times 10^4$	63.7
20	1450	25	40	$1.81 \times 10^4$	68.7

spectrum is assumed to be strongly peaked in the  $x$  and  $y$  directions, and  $a$  is the amplitude of these undulations. Note that the undulation is assumed only on one side of the magnetic layer in the above derivation. In the TEM cross sectional images,  $\lambda_y$  was around 10 nm. If we assume a factor of 1.5 greater wavelength in the easy axis ( $\lambda_x=15$  nm),  $H_K^*$  can be calculated, as listed in Table I. Comparing between  $H_K$  and  $H_K^*$ , the origin of the high anisotropy may be attributed to the anisotropic interface morphology caused by the oblique deposition of the Ru underlayer.

Annealing was performed at  $400^\circ\text{C}$  for 30 min in vacuum without a magnetic field. No significant change in the magnetic anisotropy was observed after the annealing. Lithographical process tolerance was also checked by making the films into circular cylindrical cells with diameters ranging from 400 to 200 nm by means of the electron beam lithography and Ar ion milling. Figure 4 shows the hysteresis loop for circular cylinders with diameter of 400 nm when the magnetic field is applied along the easy axis. The hysteresis loop in individual elements was measured by the magneto-optical Kerr effect (MOKE). As shown in Fig. 4(a), the squareness ratio of the hysteresis loop decreases with increasing thickness. The micromagnetic simulation of the elements was performed using the commercial code "LLG".<sup>21</sup>

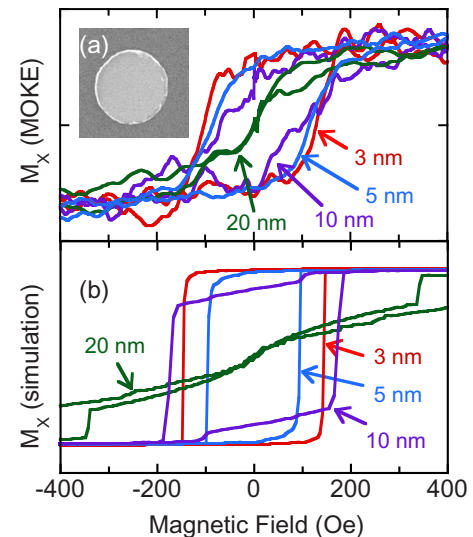


FIG. 4. (Color online) Magnetization curves of circular cylinders ( $d=400$  nm) for samples with various CoFe thicknesses when the magnetic field is applied parallel to the easy axis. (a) MOKE results and (b) micromagnetic simulation results. The inset shows the scanning electron microscopy picture of the element.

The parameters used were an exchange stiffness constant of  $1.6 \times 10^{-6}$  ergs/cm, a Gilbert damping constant of 1.0 so that the precession dies down quickly, and the  $M_S$  and  $H_K$  values listed in Table I. The simulation results, as shown in Fig. 4(b), show that for  $t=10$  and 20 nm, vortices come into play in the magnetization reversal. The coercivities obtained by simulation for  $t=3$  and 5 nm were 140 and 94 Oe, respectively, while those obtained by the MOKE measurement were 115 and 87 Oe, suggesting that the anisotropy constant may not be affected by the lithographical processes. We also detected the MOKE signals for some of the 200 and 300 nm elements, and no degradation of the magnetic anisotropy was observed. The thermal stability factor of the 100 nm elements of our thin films is also listed in Table I. All the elements maintain an activation energy sufficient for memory application ( $>60k_B T$ ), although the thicker (10 and 20 nm) films may not be suitable due to the presumed non-single-domain-like behavior mentioned above.

While the above presentation was focused on the films of  $\text{Co}_{90}\text{Fe}_{10}$ , obliquely sputtered Ru underlayers have a potential to be applied to any other magnetic materials. We obtained  $H_K$  as high as 1 kOe ( $K_u \sim 6 \times 10^5$  ergs/cm<sup>3</sup>) exhibiting similar hysteresis curve characteristics by employing this technique to  $\text{Co}_{10}\text{Fe}_{90}$ .<sup>22</sup> In summary, we have found that CoFe films can be formed with a high uniaxial magnetic anisotropy with very little hysteresis in the hard axis direction by normal incidence sputtering on top of a Ru underlayer deposited by oblique incidence sputtering. The CoFe films show no substantial degradation of the magnetic anisotropy by annealing and lithographical process. Therefore, the obliquely deposited Ru layer in the thickness range of a few nanometers will make a good underlayer for obtaining CoFe films useful for future high density, high frequency device applications.

We thank Y. Otani and T. Kimura for the help with the MOKE measurements. This work was supported in part by the National Science Foundation MRSEC Grant No. DMR-0213985. Y.F. is supported by JSPS Postdoctoral Fellowships for Research Abroad.

- <sup>1</sup>T. Klemmer, D. Hoydick, H. Okumura, B. Zhang, and W. A. Soffa, *Scr. Metall. Mater.* **10-11**, 1793 (1995).
- <sup>2</sup>T. Suzuki, *J. Magn. Soc. Jpn.* **29**, 1016 (2005).
- <sup>3</sup>T. G. Knorr and R. W. Hoffman, *Phys. Rev.* **113**, 1039 (1959).
- <sup>4</sup>D. O. Smith, *J. Appl. Phys.* **30**, S264 (1959).
- <sup>5</sup>F. G. West, *J. Appl. Phys.* **35**, 1827 (1964).
- <sup>6</sup>T. Hashimoto, K. Hara, K. Okamoto, T. Hashimoto, and H. Fujiwara, *J. Magn. Soc. Jpn.* **43**, 1415 (1973).
- <sup>7</sup>Y. Hoshi, E. Suzuki, and M. Naoe, *J. Appl. Phys.* **79**, 4945 (1996).
- <sup>8</sup>J. M. Alameda, F. Carmona, F. H. Salas, L. M. Alvarez-Prado, R. Morales, and G. T. Perez, *J. Magn. Magn. Mater.* **154**, 249 (1996).
- <sup>9</sup>H. Ono, M. Ishida, M. Fujinaga, H. Shishido, and H. Inaba, *J. Appl. Phys.* **74**, 5124 (1993).
- <sup>10</sup>S. van Dijken, G. Di Santo, and B. Poelsema, *Phys. Rev. B* **63**, 104431 (2001).
- <sup>11</sup>R. D. McMichael, C. G. Lee, J. E. Bonevich, P. J. Chen, W. Miller, and W. F. Egelhoff, Jr., *J. Appl. Phys.* **88**, 5296 (2000).
- <sup>12</sup>M. J. Hadley and R. J. Pollard, *J. Appl. Phys.* **92**, 7389 (2002).
- <sup>13</sup>Z. Zhao, P. Mani, G. J. Mankey, G. Gubbiotti, S. Tacchi, F. Spizzo, W.-T. Lee, C. T. Yu, and M. J. Pechan, *Phys. Rev. B* **71**, 104417 (2005).
- <sup>14</sup>M. T. Umlor, *Appl. Phys. Lett.* **87**, 082505 (2005).
- <sup>15</sup>A. Lisfi, J. C. Lodder, H. Wormeester, and B. Poelsema, *Phys. Rev. B* **66**, 174420 (2002).
- <sup>16</sup>M. Mao, A. J. Devasahayam, J. C. S. Kools, J. Wang, and C. Su, *J. Appl. Phys.* **93**, 8403 (2003).
- <sup>17</sup>H. B. Nie, S. Y. Xu, C. K. Ong, Q. Zhan, D. X. Li, and J. P. Wang, *Thin Solid Films* **440**, 35 (2003).
- <sup>18</sup>R. Gupta and M. Gupta, *Phys. Rev. B* **72**, 024202 (2005).
- <sup>19</sup>See EPAPS supplementary material at <http://dx.doi.org/10.1063/1.3223538> for high  $H_K$  up to 1 kOe and for TEM and XRR results.
- <sup>20</sup>E. Schlomann, *J. Appl. Phys.* **41**, 1617 (1970).
- <sup>21</sup>M. Scheinfein, <http://llgmicro.home.mindspring.com>.
- <sup>22</sup>Z. Lu, Y. Fukuma, W. H. Butler, H. Fujiwara, G. J. Mankey, and S. Matsunuma, *IEEE Trans. Magn.* **45**, 4008 (2009).